Technobius, 2026, 6(3), 0108, DOI: https://doi.org/10.54355/tbus/27897338.6.3.2026.0108

Technobius

https://technobius.kz/

e-ISSN 2789-7338

Article

Indoor extension of an inverse acoustic SPL model: a direct-reverberant field correction for multi-pattern construction noise

Shyngys Zharassov, Alisher Imanov*

Department of Civil Engineering, L.N. Gumilyov Eurasian National University, Astana, Kazakhstan
*Correspondence: glad.alisher@gmail.com

Abstract. Construction-noise propagation models are typically formulated and validated outdoors, under free-field (FF) conditions, and for a single temporal noise pattern (most often impulsive pile-driving noise). Neither assumption holds for construction and renovation work carried out inside occupied buildings, where reflected sound energy accumulates in the enclosed volume and the operating equipment may be steady, fluctuating, intermittent, or impulsive. This study extends a previously validated outdoor inverse acoustic sound pressure level (SPL) model, based on FF spherical spreading, to indoor conditions by superposing a direct and a reverberant sound field, and tests the extended model against four canonical construction-noise temporal patterns (constant, fluctuating, intermittent, impulsive) reproduced from real recordings and measured simultaneously at five synchronized receiver positions (0.1–6 m) in an enclosed conference hall. The FF model, applied unmodified indoors, showed systematic near-field under-prediction and far-field over-prediction (mean absolute error, MAE, 3.7–6.4 dB), the signature of an unmodelled reverberant field. The direct–reverberant model removed this systematic bias and reduced in-sample MAE by 63–70% and out-of-sample (leave-one-receiver-out) MAE by 56–66%. The fitted effective room constant was physically consistent and source-independent for temporally continuous sources (implied mean absorption coefficient $\bar{\alpha} \approx 0.28$–$0.30$, plausible for the hall's construction), but not for the sparse-duty-cycle intermittent source, for which the reverberant field evidently had insufficient time to establish. Counter-intuitively, recovering distance from SPL alone was less accurate with the better-fitting reverberant model than with the FF baseline, because the fitted critical distances (0.57–1.90 m) place most of the measured range in the reverberant-dominated, distance-invariant zone. The results indicate that indoor construction-noise assessment requires an explicit reverberant-field correction, that this correction depends on the source's temporal duty cycle, and that improved level-reconstruction accuracy does not, by itself, imply improved acoustic localization accuracy indoors.

Keywords: construction noise, indoor sound propagation, reverberant field, room constant, sound pressure level, inverse acoustic model, synchronized multi-receiver measurement.

1. Introduction

Construction activities are among the most variable and disruptive sources of environmental noise in urban areas because their location, duration, equipment composition, and operating conditions change continuously over the project lifecycle [1]. Objective measurements and resident surveys have shown that construction noise can dominate the local acoustic environment and produce substantially greater annoyance than other nearby sources [1], and similar concerns have been reported for rail-transit construction and other urban construction projects [2], [3], [4]. The great majority of this literature, however, concerns activities on open sites, where propagation is reasonably approximated as free-field (FF) spherical spreading, modified by ground effects, atmospheric absorption, and meteorological refraction [5], [6]. Comprehensive engineering propagation models such as Harmonoise represent these mechanisms explicitly [7], but they, too, are formulated for outdoor propagation. Impulsive construction sources such as pile driving have similarly been characterized by multi-distance field measurement in other propagation media, underscoring the general value of measuring at several distances simultaneously when validating propagation assumptions [8].

Construction and renovation work carried out inside occupied or partially occupied buildings (demolition, interior fit-out, mechanical or structural rework near finished spaces) is common in practice but has received comparatively little targeted acoustic-propagation study. Indoors, a substantial fraction of the radiated acoustic energy is reflected one or more times from the surrounding surfaces before reaching a receiver, so that beyond a certain distance from the source the sound field is dominated by this reflected (reverberant) energy rather than by the direct, geometrically spreading wave. This direct-to-reverberant transition is well established in room-acoustics theory [9], where the total sound pressure level (SPL) at distance r from a source is represented as the energetic superposition of a direct term, decaying with distance, and a reverberant term that is approximately uniform throughout the room; refinements to the classical formulation for rooms with non-uniformly distributed absorption have also been proposed [10]. None of the outdoor construction-noise propagation literature reviewed above incorporates this mechanism, because it does not arise in an open-site context.

A separate line of work has sought to predict construction-noise exposure once source and receiver locations are known. Early studies treated the measured signal as a stochastic process and used regression-based functional expansions to predict its temporal variation and associated uncertainty [10], later relating equivalent noise exposure to equipment flows, operating conditions, and source–receiver distance with a reported standard error of approximately 2 dB(A) [11]. Simulation-based approaches subsequently incorporated construction sequencing, multiple simultaneously operating sources, and energy-based equivalent-level calculation [12], reporting differences between predicted and measured levels on the order of 1.2–2.8 dB(A) [13], [14]. More recent work has moved toward real-time sensing and data-driven spatial interpolation, combining measured data with ISO 9613-2-based [15] propagation modelling and reporting root-mean-square error (RMSE) values around 2.6–2.7 dB [16]. These methods are valuable for exposure prediction at known, predetermined receiver and source positions, but, like the outdoor propagation literature above, none addresses an enclosed, reflection-dominated environment or more than a single, usually steady or impulsive, noise character.

Sound-source localization has also been studied extensively outside the construction-management field, generally using microphone arrays, waveform timing, or phase information: acoustic beamforming [17], time-reversal processing requiring a numerical propagation model of the surroundings [18], reflection-aware localization using reconstructed room geometry [19], and finite-element or sparse inverse reconstruction schemes requiring transfer functions and regularization [20], [21]. These approaches can achieve high spatial resolution but require instrumentation and environmental information well beyond a handful of simple sound level meters.

Against this background, a transparent inverse acoustic model was recently developed and field-tested for locating an unknown pile-driving source and reconstructing its time-varying SPL from five synchronized, GNSS-positioned sound level meters on an open construction site [22]. That model assumes pure spherical spreading (appropriate given the site's open, unobstructed geometry) and jointly estimates source position and a time-varying source level by minimizing the disagreement among distance-corrected source-level estimates from the five receivers. Applied to a single pile-driving event, it achieved a localization error of 2.3 m against an independently surveyed ground-truth position and an overall SPL-reconstruction mean absolute error (MAE) of 1.3 dB(A) and RMSE of 1.6 dB(A). Its authors explicitly identified two directions for extension: testing the model against source types other than impulsive pile-driving noise, and testing it under propagation conditions beyond the open, reflection-free site on which it was validated [22]. A separate, earlier pilot study compared pulsed, steady, and blended sound sources at four short-range posts (0–3 m) using single-device video-timestamp reading of the sound level meter display, but its lack of true multi-device synchronization limited it to per-device analysis and prevented the kind of joint multi-receiver inversion used in [22]; that pilot study also did not incorporate an enclosed-space (reverberant) propagation term [23].

The present study addresses both extensions simultaneously. SPL measurements were carried out indoors, in an enclosed conference hall, using five synchronized UT352 sound level meters at radial distances of 0.1–6 m from a loudspeaker reproducing four pre-recorded construction-noise tracks representing canonical temporal patterns (constant, fluctuating, intermittent, and impulsive) rather than a single impulsive source. Time-to-time synchronization across the five independently filmed receivers was achieved with the RecSyncNG multi-device synchronization application [24], directly resolving the single-device timestamp-matching limitation of [23]. The FF inverse model of [22] is extended by superimposing a reverberant-field term following the classical room-acoustics formulation [9], [10], and the extended model is fitted, cross-validated, and compared against the unmodified FF model using the same reconstruction-error and out-of-sample procedures as [22].

Accordingly, this study aims to: (i) test whether the FF geometrical-spreading model of [22] remains valid for indoor construction-noise propagation; (ii) develop and validate a direct–reverberant field extension of that model; (iii) test whether the extension generalizes across constant, fluctuating, intermittent, and impulsive noise sources, and whether its fitted room-acoustic parameter behaves as a physically consistent, source-independent property of the room; and (iv) examine whether improvements in SPL-reconstruction accuracy translate into improved distance-recovery (localization) accuracy indoors.

2. Methods

2.1 Indoor field measurements

Measurements were conducted in an enclosed conference hall (elliptical floor plan, major and minor diameters 15 m and 10 m; L.N. Gumilyov Eurasian National University, Astana, Kazakhstan) under closed, quiet conditions. A Bluetooth loudspeaker was positioned at the geometric center of the hall (Figure 1) and played back four pre-recorded audio tracks representing canonical construction-noise temporal patterns: 1) constant (generator running); 2) fluctuating (concrete mixing); 3) intermittent (hammer on wood); 4) impulse (pile driving). The loudspeaker was controlled remotely by Bluetooth from outside the hall so that no operator was present in the room during playback.

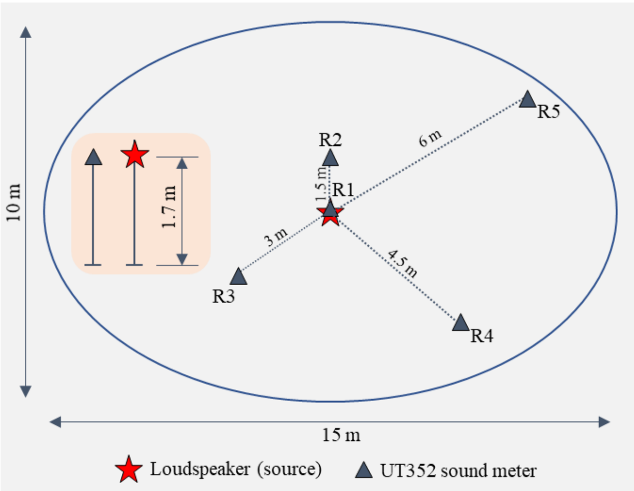

Figure 1 – Schematic plan of the conference hall (ellipse, 15 × 10 m) showing the loudspeaker (source) at the center and the five UT352 receiver positions at their measured radial distances (the angular arrangement of the receivers around the source is illustrative, since only radial distance was recorded for each); all source and receiver positions were coplanar at 1.7 m height

Five UT352 sound level meters (UNI-T, Dongguan, China; A-weighting, FAST time response, 0.125 s sampling interval, 8 records per second, 30–130 dB range, ±1.5 dB accuracy) were mounted on purpose-built stands (Figure 2) at radial distances of 0.1, 1.5, 3, 4.5, and 6 m from the source. The loudspeaker and all five microphones were fixed at the same height of 1.7 m above the floor, so the source and all receivers were coplanar; the nominal radial distances therefore equal the true source-to-receiver distances, and no vertical-offset correction is required, unlike the outdoor pile-driving measurements of [22], where source and receiver heights differed.

Figure 2 – Measurement setup: R1-R5 – receivers

For each of the four audio tracks, a representative 5 s segment was extracted, and the corresponding UT352 screen readings were recorded at all five receivers simultaneously. Time-to-time synchronization across the five independently filmed devices was ensured using the RecSyncNG Android application [24], which provides frame-accurate multi-device synchronization and thereby resolves the single-device timestamp-matching limitation of the earlier pilot study [23]. Each 5 s segment yielded 40 SPL readings per receiver (0.125 s intervals), i.e., 200 measurements per noise type (5 receivers × 40 time steps). All SPL values are A-weighted levels referenced to 20 µPa (dB(A)), consistent with the UT352 operating mode.

2.2 Sound propagation model: direct and reverberant field superposition

The outdoor model of [22] assumes pure spherical (FF) spreading, appropriate for an open site with unobstructed line of sight. An enclosed room additionally returns reflected acoustic energy to the receiver; once the source has operated long enough, relative to its own duty cycle, for reflections to accumulate, the sound field at distance r from a point source is commonly represented as the superposition of a direct field and a reverberant field, approximately uniform throughout the room [9]:

$$L_p(r) = L_w + 10log_{10}\left(\frac{Q}{4\pi r^2} + \frac{4}{R}\right), \quad (1)$$

where: L_w is the source sound power level, Q is the source directivity factor, and R is the room constant (m^2), $R = \frac{S\bar{\alpha}}{1-\bar{\alpha}}$ with S the total interior surface area and $\bar{\alpha}$ the surface-averaged absorption coefficient. The distance at which the direct and reverberant terms are equal (the critical distance) is:

$$r_c = \sqrt{\frac{QR}{16\pi}}, \quad (2)$$

To keep the reference quantity directly comparable with the outdoor model, $L_{s,k}$ is defined, as in [22], as the extrapolated FF level at reference distance r_0 = 1 m (i.e., the level Eq. (1)) would give at r_0 in the limit as R tends to infinity). Substituting $L_{s,k} = -10log_{10}\left(\frac{Q}{4\pi}\right)$ into Eq. (1) gives the working form used throughout this study:

$$L_{i,k}^{meas,c} = L_{s,k}^{c} + 10log_{10}\left(\frac{1}{r_i^2} + \frac{16\pi}{R_{eff}}\right) + \varepsilon_{i,k}, \quad (3)$$

with r_0 = 1 m, $R_{eff} \equiv R{\cdot}Q$, i = 1,…,5 (receiver), k = 1,…,40 (time step), and $c \in$ {Constant, Fluctuating, Intermittent, Impulse}. Because the measurement geometry used here (single source height, coplanar receivers) cannot separately resolve R and Q, only their product is identifiable from the data; R_{eff} is therefore reported and interpreted throughout as an effective room constant, not a directly measured, absorption-based R. As R_{eff} tends to infinity, this recovers the outdoor FF model of [22]:

$$L_{i,k}^{meas,c} = L_{s,k}^{c} - 20log_{10}\left(\frac{r_i}{r_0}\right) + \varepsilon_{i,k}, \quad (4)$$

Eq. (4) (fixed exponent of 20, i.e., n = 2) is retained unmodified as the FF baseline against which Eq. (3) is compared, rather than a floated-exponent power law, so that the comparison isolates the effect of adding the reverberant term rather than simply allowing an extra free parameter.

2.3 Inverse estimation of the effective room constant and source SPL

Receiver coordinates (and hence distances r_i) are known by construction in this controlled indoor experiment, unlike the outdoor pile-driving case of [22], where source position was unknown. The unknowns here are the effective room constant R_{eff} (assumed constant over the 5 s window and shared across all five receivers) and the time-varying source level $L_{s,k}^{c}$. For an assumed value of R_{eff}, the back-calculated source level from receiver i at step k is obtained by inverting Eq. (3):

$$L_{s,i,k}(R_{eff}) = L_{i,k}^{meas,c} - 10log_{10}\left(\frac{1}{r_i^2} + \frac{16\pi}{R_{eff}}\right) + \varepsilon_{i,k}, \quad (5)$$

and the consensus source level at step k is the across-receiver mean:

$$L_{s,k}(R_{eff}) = \frac{1}{5}\sum_{i=1}^{5} L_{s,i,k}(R_{eff}), \quad (6)$$

Analogously to the position search of [22], the optimal R_{eff} is the value minimizing the across-receiver disagreement in the back-calculated source level, summed over all receivers and time steps:

$$J(R_{eff}) = \sum_{k=1}^{40}\sum_{i=1}^{5}\left[L_{s,i,k}(R_{eff}) - L_{s,k}(R_{eff})\right]^2, \quad (7)$$

$$R_{eff} = argmin_{R_{eff}} J(R_{eff}), \quad (8)$$

solved by bounded scalar minimization over $R_{eff} \in [0.2, 20000]$ m^2. The corresponding source-level time history $L_{s,k}^*$ is obtained by substituting R_{eff}^* into Eqs. (5) and (6), and the equivalent source SPL over the 5 s window follows the same energy-averaging definition used in [22]:

$$L_{s,eq} = 10log_{10}\left(\frac{1}{40}\sum_{k=1}^{40} 10^{L_{s,k}^*/10}\right), \quad (9)$$

The FF baseline (Eq. (4)) is fitted the same way, with the $20_{log10}(r_i/r_0)$ term in place of Eq. (5). This formulation was applied both to each noise type separately and pooled across the three temporally continuous types (Constant, Fluctuating, Impulse) with a shared R_{eff}, to test whether the fitted room constant behaves as a source-independent physical property of the room.

2.4. Reconstruction consistency check

Predicted receiver levels were computed from R_{eff}^* and $L_{s,k}^*$ and compared with measured levels; MAE and RMSE were computed exactly as in [22], separately for the reverberant model (Eq. (3)) and the FF baseline (Eq. (4)). Per-receiver signed (mean) error was also computed to check for residual distance-dependent bias, since a systematic bias trend with distance would indicate propagation-model misspecification rather than random measurement scatter.

2.5. Out-of-sample cross-validation and distance-recovery test

Following the leave-one-receiver-out (LORO) procedure of [22], R_{eff} and $L_{s,k}$ were re-estimated using only four of the five receivers, and the held-out receiver's measured SPL (never used in that fit) was predicted from the resulting estimate; this was repeated with each of the five receivers held out in turn, for both models.

Because the receiver geometry is known here, an additional out-of-sample test (a distance-recovery test) was performed: for each held-out receiver and time step, the fitted model was inverted to solve for the implied distance $\hat{r}$ from the held-out receiver's measured SPL and the $L_{s,k}$, R_{eff} estimated from the remaining four receivers, and compared with the known true distance. For the reverberant model, inversion of Eq. (3) gives:

$$\hat{r} = \left[10^{\frac{L-L_{s,k}}{10}} - \frac{16\pi}{R_{eff}}\right]^{-\frac{1}{2}}, \quad (10)$$

which is only real-valued when the bracketed term is positive, i.e., when the observed level lies above the reverberant floor implied by R_{eff}. When this condition fails, the inversion is capped at an upper bound (15 m, the approximate room half-diagonal) rather than discarded, so that no cases are silently excluded from the reported distance-error statistics. The FF model is inverted analogously ($\hat{r} = 10^{\frac{L_{s,k}-L}{20}}$), which is always resolvable. The distance-recovery test is a more demanding, and physically distinct, validation than the SPL-reconstruction MAE/RMSE: it directly probes whether the fitted model supports ranging, not merely level prediction.

2.6. Sensitivity and Uncertainty Analysis

The sensitivity of R_{eff} to SPL measurement uncertainty was assessed by perturbing the measured SPL with independent, zero-mean Gaussian noise (σ_L = 1.5 dB, matching the manufacturer-specified accuracy of the UT352) and re-estimating R_{eff} for each of 1000 realizations, following the procedure of Section 2.3. The standard deviation and 95% percentile interval of the resulting R_{eff} and $r_c = \sqrt{\frac{R_{eff}}{16\pi}}$, distributions are reported for each noise type.

A pooled-versus-individual hypothesis test compared the individually fitted R_{eff} for Intermittent noise against the pooled R_{eff} of the three continuous-type sources, using a z-statistic based on the Monte Carlo standard errors of each:

$$z = \frac{R_{eff,Intermittent} - R_{eff,pooled}}{\sqrt{SE^2_{Intermittent} + SE^2_{pooled}}}, \quad (11)$$

Finally, as an approximate, independent physical-plausibility check (not used to constrain the data-driven fit itself), the surface-averaged absorption coefficient $\bar{\alpha}$ implied by each fitted R_{eff} was back-calculated as $\bar{\alpha} = \frac{R_{eff}}{S+R_{eff}}$, using the known elliptical floor area (15 × 10 m; $A = \pi ab$ = 117.8 m^2) and an assumed ceiling height (3.0–4.0 m range tested) to estimate the total interior surface area S (floor + ceiling + walls, via the ellipse perimeter). No room-surface absorption coefficients or measured reverberation time were available for this hall; the check therefore tests only whether the fitted R_{eff} values are of a physically reasonable order of magnitude for the given room geometry.

2.7. Signal Temporal-Pattern Descriptors

To characterize each source track's temporal structure independently of the measured SPL data, the original .wav recordings (48 kHz) were segmented into the same 0.125 s windows as the UT352 sampling interval, and per-window RMS level was computed after averaging stereo channels to mono. The standard deviation and full range of the RMS-level envelope across the complete track (21–52 s duration; longer than the 5 s excerpt used for the SPL measurements) served as objective duty-cycle ("burstiness") descriptors, used in Section 3 to interpret differences in fitted R_{eff} between noise types. These are uncalibrated digital full-scale (FS) levels (dBFS) and are not equivalent to, nor substitutable for, the acoustic UT352 SPL measurements; they are used only in a relative, within-track sense.

3. Results and Discussion

Table 1 summarizes the energy-equivalent SPL at each of the five receiver distances for the four noise types. In contrast to the outdoor pile-driving measurements of [22], where equivalent SPL decreased monotonically with distance at all five receivers, the indoor data show a markedly different pattern: after an initial decrease from 0.1 to 1.5 m, the equivalent SPL is flat or non-monotonic across the 1.5–6 m range for three of the four noise types (e.g., Constant: 66.0 dB(A) at 1.5 m versus 66.6 dB(A) at 3 m). This is the expected signature of a direct-to-reverberant field transition in an enclosed space, and it already indicates that an FF model cannot be applied indoors without modification.

Table 1 – Energy-equivalent SPL (at each receiver distance, all five posts, per noise type), dB(A) re 20 μPa

Noise type	0.1 m	1.5 m	3 m	4.5 m	6 m
Constant	88.4	66.0	66.6	63.8	61.4
Fluctuating	91.8	69.3	69.5	67.8	65.7
Intermittent	82.8	66.8	66.2	65.8	60.5
Impulse	85.5	63.3	65.6	61.6	59.9

Fitting the reverberant model (Eq. (3)) and outdoor FF baseline (Eq. (4), $n = 2$ fixed) to the full time-resolved dataset (200 measurements per type: 5 receivers × 40 time steps) confirms this: the reverberant model reduced in-sample MAE by 63–70% and RMSE by 51–63% relative to the FF baseline across all 4 noise types, and out-of-sample MAE by a further 56–66% (Table 2). Figure 3 directly shows that the fitted reverberant curve tracks the measured points across the full 0.1–6 m range for every noise type, while the FF curve only fits well near the source for every noise type.

Table 2 – Forward-model comparison (all five receivers, coplanar (1.7 m) geometry: fitted parameters, in-sample reconstruction accuracy, and LORO out-of-sample accuracy, reverberant model versus FF baseline)

Noise type	R_{eff}, m^2	r_c, m	In-sample MAE / RMSE, rev., dB	In-sample MAE / RMSE, FF, dB	LORO MAE / RMSE, rev., dB	LORO MAE / RMSE, FF, dB
Constant	182.0	1.90	1.10 / 1.40	3.71 / 3.82	1.59 / 2.00	4.63 / 4.77
Fluctuating	150.1	1.73	1.08 / 1.27	3.92 / 4.14	1.64 / 1.88	4.90 / 5.18
Intermittent	16.4	0.57	2.79 / 3.94	6.35 / 8.00	3.49 / 5.37	7.94 / 9.99
Impulse	131.6	1.62	2.08 / 2.64	4.35 / 4.84	3.05 / 3.70	5.43 / 6.05

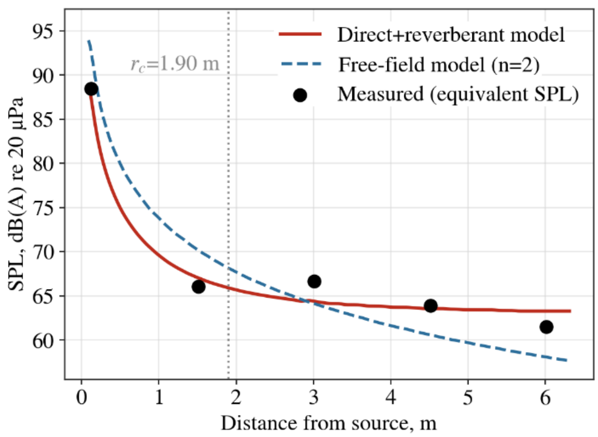

a) Constant (generator running)

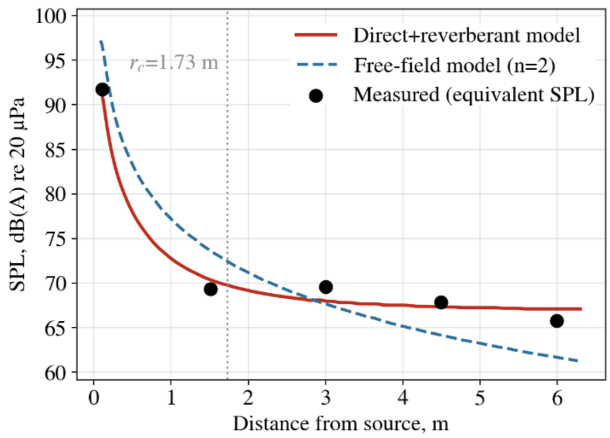

b) Fluctuating (concrete mixing)

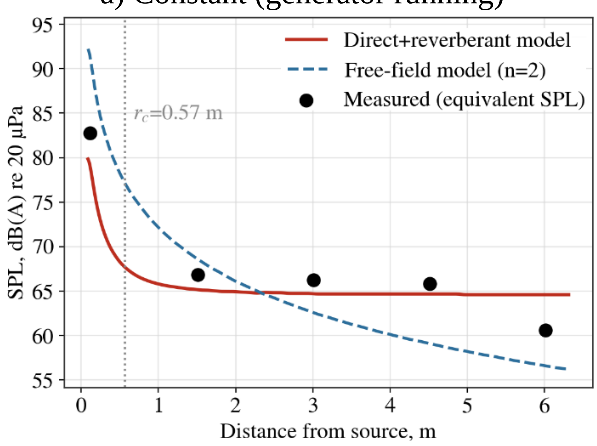

c) Intermittent (hammer on wood)

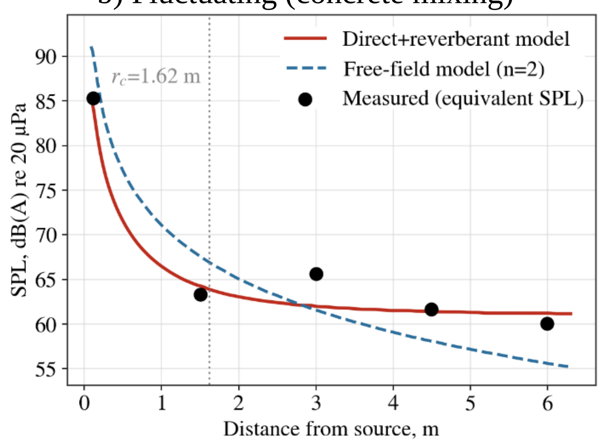

d) Impulse (pile driving)

Figure 3 – Measured equivalent SPL (points) versus the fitted reverberant model (solid) and FF model (dashed), by noise type (vertical dotted line marks the fitted critical distance r_c for each type)

This margin is directly comparable, in order of magnitude, to the reconstruction accuracy reported for the outdoor pile-driving model itself (MAE 1.3 dB(A), RMSE 1.6 dB(A) [22]) and to other construction-noise prediction studies that report errors in the 1.2–2.8 dB(A) range under their own, generally outdoor, conditions [11], [13], [14], [16]. The present indoor reverberant-model MAE (1.1–2.8 dB) falls within, or close to, that same range for three of the four noise types, indicating that an appropriately corrected indoor model can match the accuracy achieved outdoors, whereas the uncorrected FF model (3.7–6.4 dB) cannot.

The mechanism is visible directly in the per-receiver signed bias: the FF model systematically under-predicts the near receivers (−4.1 to −12.4 dB at 0.1–1.5 m, across the four noise types) and over-predicts the far receivers (+1.9 to +7.0 dB at 3–6 m), the classic signature of an unmodelled reverberant contribution described in the room-acoustics literature [9], [10]. The reverberant model shows no such systematic trend; its residual bias at each distance is generally below 2.5 dB and does not show a consistent sign progression with distance, indicating that the direct-reverberant superposition, rather than random measurement scatter, is what the FF model was missing.

The distance-recovery test shows the opposite ranking from the SPL-reconstruction test (Figure 4b): the FF model recovers the true receiver distance more accurately (mean error 1.25–1.78 m, out-of-sample) than the reverberant model (mean error 2.42–4.48 m), despite reconstructing SPL levels substantially worse. This apparent contradiction is explained by the fitted critical distances (Table 2, r_c = 0.57–1.90 m): for the continuous-type sources, r_c is smaller than the 1.5 m spacing of the nearest four receivers, so almost the entire 1.5–6 m measurement range lies beyond r_c, where the reverberant term of Eq. (1) dominates and SPL becomes nearly independent of distance. In this regime, SPL-to-distance inversion is intrinsically ill-conditioned: a small SPL error maps to a large distance error, regardless of how accurately the forward model reconstructs levels. FF model's rigid, monotonic $20log_{10}(r)$ relationship, while a poorer level predictor overall, remains uniquely invertible everywhere and is therefore less sensitive to this ill-conditioning. This has a direct bearing on the localization literature reviewed in Section 1 [17], [18], [19], [20], [21]: those methods achieve high spatial resolution primarily by exploiting phase, array geometry, or explicit reflection paths, precisely because scalar-level information alone becomes uninformative about distance beyond the critical distance in a reverberant space. The present result quantifies that limit for a simple, low-cost, scalar-SPL method and shows that it is a property of the acoustic field itself, not merely of model choice: improving level-reconstruction accuracy does not imply improved localization accuracy indoors.

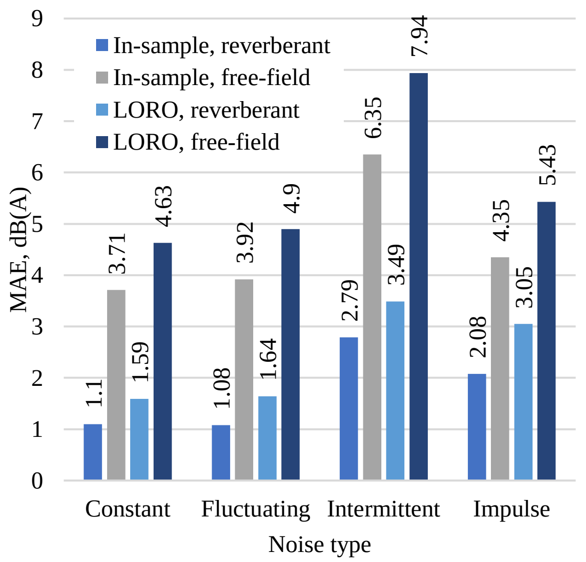

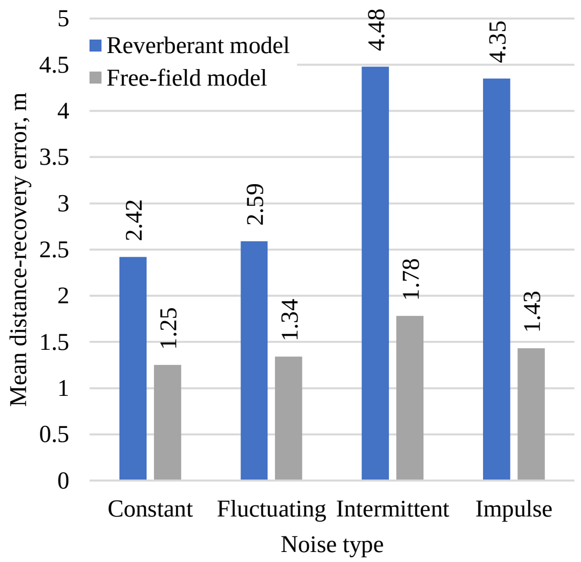

a) b)

Figure 4 – SPL-reconstruction and distance-recovery accuracy (reverberant versus FF model, by noise type)

Monte Carlo perturbation of the measured SPL (σ_L = 1.5 dB, matching UT352 accuracy, 1000 realizations) gave well-constrained R_{eff} estimates for all four noise types: Constant 181.5 ± 14.2 m^2 (r_c = 1.90 ± 0.07 m), Fluctuating 151.0 ± 10.6 m^2 (r_c = 1.73 ± 0.06 m), Intermittent 16.4 ± 1.1 m^2 (r_c = 0.57 ± 0.02 m), and Impulse 132.2 ± 9.5 m^2 (r_c = 1.62 ± 0.06 m); relative standard deviations of 6–8% throughout. R_{eff} is therefore a stable, well-conditioned fit parameter under realistic instrument-accuracy noise, and is not primarily an artifact of measurement uncertainty.

If R_{eff} behaves as a genuine, source-independent property of the room, pooling data across noise types with a shared R_{eff} should be consistent with the individually fitted values. Pooling the three continuous-type sources (Constant, Fluctuating, Impulse) gave R_{eff} = 152.6 m^2 (r_c = 1.74 m), within the range of the three individual fits (132–182 m^2) and consistent with all three at the level of their Monte Carlo uncertainty above. Intermittent noise is a clear outlier: its individually fitted R_{eff} (16.4 ± 1.1 m^2) differs from the pooled continuous-type value by $z = -11.85$ (Eq. (11)), far exceeding the $|z| > 2$ threshold for 95% distinguishability.

A physical-plausibility check clarifies the likely cause. Using the known elliptical floor area (15 × 10 m; A = 117.8 m^2) and an assumed ceiling height in the 3.0–4.0 m range, the pooled continuous-type R_{eff} implies a surface-averaged absorption coefficient $\bar{\alpha}$ of approximately 0.28–0.30 (rising to 0.30 at the lower height assumption, falling to 0.28 at the higher one), a physically reasonable value for a hard-floored, painted-wall, suspended-tile-ceiling lecture hall of the kind visible in Figure 2. Intermittent's fitted R_{eff} , by contrast, implies $\bar{\alpha}$ of approximately 0.04 across the same height range, implausibly low for any real interior surface combination. This indicates that the low R_{eff} fitted for Intermittent should not be interpreted as a physically meaningful room-absorption estimate; rather, it reflects the fitting procedure compensating for a source whose energy is too sparse in time to establish a representative reverberant field within the 5 s analysis window.

This interpretation is supported directly by the source recordings' own temporal statistics. Segmenting each full-length .wav track (21–52 s, longer than the 5 s SPL excerpt) into 0.125 s windows and computing the RMS-level envelope shows Intermittent to have a far larger standard deviation (17.3 dB) and range (66.7 dB) than the other three tracks (0.2–7.4 dB and 1.6–29.1 dB, respectively; mean crest factors 12.0–15.7 dB across all four), reflecting long near-silent intervals interrupted by brief, high-amplitude hammer strikes. Within the 5 s measurement window, this low duty cycle leaves little time for reflected energy to build up to a steady reverberant level before the source characteristic changes again, a plausible, though not separately tested, physical explanation for Intermittent's anomalously low and physically implausible fitted R_{eff}. This complements the original comparison between pulsed and steady/blended sounds in [23], which found pulsed sound to have the largest close-range fluctuations of the three source types tested but did not examine indoor reverberant-field build-up specifically, since its own short-range (0–3 m), single-device measurements did not extend far enough to observe the plateau documented here (Table 1, Figure 3); nor did that study's simple exponential distance-decay fit (R^2 = 0.8664, reported over 0–3 m for the median of all sources combined) attempt to separate a direct-field from a reverberant-field contribution, which the present results show is necessary once measurements extend indoors beyond roughly 1.5–2 m.

Several limitations should be considered when interpreting these results. First, the study is limited to a single room, a single source position, and a single assumed source height (coplanar with the receivers); the generality of the fitted R_{eff} values, and of the pooled-versus-Intermittent distinction, to other rooms, source heights, or source positions relative to room boundaries has not been tested. Second, the vertical and horizontal directivity of the loudspeaker used to reproduce the source tracks was not characterized and is absorbed into the identifiability limitation of $R_{eff} = R \cdot Q$ noted in Section 2.2; a directional construction-noise source (e.g., a wall-mounted saw or a floor-coupled compactor) could behave differently. Third, the physical-plausibility check above assumes, rather than measures, the hall's ceiling height and treats the room as having uniformly distributed absorption; neither the reverberation time nor per-surface absorption coefficients were measured directly, so the implied $\bar{\alpha}$ should be read as an approximate order-of-magnitude check, not a calibrated acoustic property of the hall. Fourth, as in the outdoor model of [22], the reverberant extension presented here assumes a single dominant source and a room geometry that does not change during the measurement; simultaneous or moving sources, and irregular or partially occupied rooms with furniture or people redistributing absorption during construction work, would require further extension. Fifth, the receivers were arranged radially from the source at only five distances and unrecorded azimuths, so the model is validated only for its assumed isotropic (radial) form; a genuinely spatial (two-dimensional) picture of the indoor field, for instance by adding receivers at multiple azimuths per radius, was not attempted here, since a spatial interpolation from only five points at unrecorded angles would not be a reliable, independently validated result and was judged unhelpful to include. This is a natural direction for future work. Finally, the distance-recovery ill-conditioning identified beyond the critical distance is a property of scalar-SPL-only methods in general, including the present one and the outdoor model of [22] if applied indoors unmodified; overcoming it indoors would likely require the kind of array, phase, or reflection information used in [17], [18], [19], [20], [21], at correspondingly greater instrumentation cost.

4. Conclusions

This study extended a previously validated outdoor, FF inverse acoustic SPL model to indoor propagation, and tested the extension across four canonical construction-noise temporal patterns (constant, fluctuating, intermittent, and impulsive) measured simultaneously with five synchronized receivers in an enclosed conference hall. Four conclusions follow from the results.

First, the unmodified outdoor FF model does not transfer to indoor conditions: it showed systematic near-field under-prediction and far-field over-prediction (MAE 3.7–6.4 dB) for every noise type tested, the expected signature of an unmodelled reverberant field. Second, superposing a direct and reverberant field term, following classical room-acoustics theory, removed this systematic bias and reduced SPL-reconstruction error by 63–70% in-sample and 56–66% out-of-sample, bringing indoor reconstruction accuracy back into the same range reported for the outdoor model itself and for other construction-noise prediction studies. Third, the fitted effective room constant behaved as a physically consistent, source-independent property of the room for temporally continuous sources (pooled R_{eff} = 152.6 m^2, implying a plausible mean absorption coefficient of $\bar{\alpha} \approx$ 0.28–0.30), but not for the sparse-duty-cycle intermittent source, whose fitted R_{eff} was almost an order of magnitude smaller and implied a physically implausible $\bar{\alpha} \approx 0.04$. This discrepancy is consistent with the source recordings' own temporal statistics, which show intermittent noise to be far burstier than the other three types, leaving insufficient time within the analysis window for a representative reverberant field to develop. Fourth, and counter-intuitively, the better-fitting reverberant model was less accurate than the simpler FF model at recovering distance from SPL alone, because the fitted critical distances (0.57–1.90 m) place most of the 1.5–6 m measurement range in the reverberant-dominated, SPL-invariant zone, where distance is not recoverable from level alone regardless of forward-model quality. Improved level-reconstruction accuracy and improved localization accuracy are therefore not interchangeable objectives indoors, and this distinction should inform the design of any future indoor acoustic monitoring or localization system based on simple sound level meters.

Future work should test the extended model in additional rooms and with additional source and receiver geometries, including receivers at multiple azimuths, to test whether the fitted room constant and critical distance are isotropic; measure reverberation time and surface absorption directly rather than relying on an approximate plausibility check, and examine sources with directional radiation patterns and moving or multiple simultaneous sources, which lie outside the single-dominant-source, coplanar-geometry scope of the present study.

Acknowledgments

This research was funded by the Science Committee of the Ministry of Science and Higher Education of the Republic of Kazakhstan (Grant No. AP25794001).

References

[1] M. J. Ballesteros, M. D. Fernández, S. Quintana, J. A. Ballesteros, and I. González, "Noise emission evolution on construction sites. Measurement for controlling and assessing its impact on the people and on the environment," *Building and Environment*, vol. 45, no. 3, pp. 711–717, 2010, doi: 10.1016/j.buildenv.2009.08.011.

[2] A. Gilchrist, E. N. Allouche, and D. Cowan, "Prediction and mitigation of construction noise in an urban environment," *Canadian Journal of Civil Engineering*, vol. 30, no. 4, pp. 659–672, 2003, doi: 10.1139/l03-019.

[3] C. Zou, Zhu, Z. Tao, D. Ouyang, and Y. Chen, "Evaluation of Building Construction-Induced Noise and Vibration Impact on Residents," *Sustainability*, vol. 12, no. 4, p. 1579, 2020, doi: 10.3390/su12041579.

[4] J. Zhang, J. Huang, Z. Wu, and Z. Li, "Construction Noise Reduction Research on Rail Transit Projects: A Case Study in China," *Buildings*, vol. 14, no. 6, p. 1678, 2024, doi: 10.3390/buildings14061678.

[5] K. Attenborough, "Review of ground effects on outdoor sound propagation from continuous broadband sources," *Applied Acoustics*, vol. 24, no. 4, pp. 289–319, 1988, doi: 10.1016/0003-682X(88)90086-2.

[6] T. F. W. Embleton, "Tutorial on sound propagation outdoors," *The Journal of the Acoustical Society of America*, vol. 100, no. 1, pp. 31–48, 1996, doi: 10.1121/1.415879.

[7] E. Salomons, D. Van Maercke, J. Defrance, and F. De Roo, "The Harmonoise Sound Propagation Model," *Acta Acustica united with Acustica*, vol. 97, no. 1, pp. 62–74, 2011, doi: 10.3813/AAA.918387.

[8] H. Bailey, B. Senior, D. Simmons, J. Rusin, G. Picken, and P. M. Thompson, "Assessing underwater noise levels during pile-driving at an offshore windfarm and its potential effects on marine mammals," *Marine Pollution Bulletin*, vol. 60, no. 6, pp. 888–897, 2010, doi: 10.1016/j.marpolbul.2010.01.003.

[9] L. L. Beranek and T. J. Mellow, "Acoustics: sound fields, transducers and vibration," 2nd ed., London, UK: Academic Press, 2019, p. 881.

[10] H. Arau-Puchades and U. Berardi, "A Revised Sound Energy Theory Based on a New Formula for the Reverberation Radius in Rooms with Non-Diffuse Sound Field," *Archives of Acoustics*, vol. 40, no. 1, pp. 33–40, Mar. 2015, doi: 10.1515/aoa-2015-0005.

[11] E. Manatakis and D. Skarlatos, "A statistical model for evaluation and prediction of the noise exposure in a construction equipment area," *Applied Acoustics*, vol. 63, no. 7, pp. 759–773, 2002, doi: 10.1016/S0003-682X(01)00073-1.

[12] H. Zhang and Y. Pei, "Simulation-Based Prediction of Equivalent Continuous Noises during Construction Processes," *International Journal of Environmental Research and Public Health*, vol. 13, no. 8, p. 818, 2016, doi: 10.3390/ijerph13080818.

[13] T. Hong, C. Ji, J. Park, S.-B. Leigh, and D. Seo, "Prediction of Environmental Costs of Construction Noise and Vibration at the Preconstruction Phase," *Journal of Management in Engineering*, vol. 31, no. 5, p. 04014079, 2015, doi: 10.1061/(ASCE)ME.1943-5479.0000313.

[14] W. C. Ooi, M. H. Lim, and Y. L. Lee, "Development of stochastic deep learning model for the prediction of construction noise," *Ain Shams Engineering Journal*, vol. 15, no. 4, p. 102592, 2024, doi: 10.1016/j.asej.2023.102592.

[15] "ISO 9613-2:2024 Acoustics - Attenuation of sound during propagation outdoors Part 2: Engineering method for the prediction of sound pressure levels outdoors," Geneva, Switzerland: ISO, 2024, p. 45.

[16] G. Lee, S. Moon, J. Hwang, and S. Chi, "Development of a real-time noise estimation model for construction sites," *Advanced Engineering Informatics*, vol. 58, p. 102133, 2023, doi: 10.1016/j.aei.2023.102133.

[17] P. Chiariotti, M. Martarelli, and P. Castellini, "Acoustic beamforming for noise source localization – Reviews, methodology and applications," *Mechanical Systems and Signal Processing*, vol. 120, pp. 422–448, 2019, doi: 10.1016/j.ymssp.2018.09.019.

[18] D. G. Albert, L. Liu, and M. L. Moran, "Time reversal processing for source location in an urban environment," *The Journal of the Acoustical Society of America*, vol. 118, no. 2, pp. 616–619, 2005, doi: 10.1121/1.1925849.

[19] I. An, M. Son, D. Manocha, and S.-E. Yoon, "Reflection-Aware Sound Source Localization," in *2018 IEEE International Conference on Robotics and Automation (ICRA)*, Brisbane, QLD, Australia: IEEE, 2018, pp. 66–73. doi: 10.1109/ICRA.2018.8461268.

[20] S. Gombots, J. Nowak, and M. Kaltenbacher, "Sound source localization – state of the art and new inverse scheme," *e & i Elektrotechnik und Informationstechnik*, vol. 138, no. 3, pp. 229–243, 2021, doi: 10.1007/s00502-021-00881-6.

[21] P. A. Nelson and S. H. Yoon, "Estimation of acoustic source strength by inverse methods: Part I, conditioning of the inverse problem," *Journal of Sound and Vibration*, vol. 233, no. 4, pp. 639–664, 2000, doi: 10.1006/jsvi.1999.2837.

[22] Y. Utepov, S. Zharassov, and F. Abdushkurov, "Inverse Acoustic Localization of Pile-Driving Noise from Synchronized Multi-Receiver SPL Measurements," *Eng*, vol. 7, no. 9, p. 439, 2026, doi: 10.3390/eng7090439.

[23] A. Imanov, A. Kozhas, A. Mukhamejanova, A. Nazarova, and D. Kazhimkanuly, "Experimental study of sound wave propagation patterns," *Technobius*, vol. 4, no. 2, p. 0057, 2024, doi: 10.54355/tbus/4.2.2024.0057.

[24] *RecSyncNG: Video Processing Tools*. (2026). Accessed: Jul. 24, 2026. [Online]. Available: https://github.com/DFKI-SignLanguage/RecSyncNG

Information about authors:
Shyngys Zharassov – PhD, Senior Lecturer, Department of Civil Engineering, L.N. Gumilyov Eurasian National University, Astana, Kazakhstan, zhshzh95@gmail.com
Alisher Imanov – PhD, Senior Lecturer, Department of Civil Engineering, L.N. Gumilyov Eurasian National University, Astana, Kazakhstan, glad.alisher@gmail.com

Author Contributions:
Shyngys Zharassov – modeling, analysis, visualization, interpretation, drafting, editing.
Alisher Imanov – resources, data collection, testing, modeling.

Conflict of Interest: The authors declare no conflict of interest.

Use of Artificial Intelligence (AI): Grammarly v1.2.297.1957 was used to improve language. The authors reviewed all the text and take full responsibility for the content of the article.

Received: 15.07.2026
Revised: 23.09.2026
Accepted: 25.09.2026
Published: 27.09.2026